TU Delft

Delft University of Technology

Numerical investigation of residual ultimate strength of dented metallic pipes subjected to pure bending

Cai, Jie; Jiang, Xiaoli; Lodewijks, Gabriel

DOI
10.1080/17445302.2018.1430200

Publication date
2018

Document Version
Final published version

Published in
Ships and Offshore Structures

Citation (APA)
Cai, J., Jiang, X., & Lodewijks, G. (2018). Numerical investigation of residual ultimate strength of dented metallic pipes subjected to pure bending. *Ships and Offshore Structures*, *13*(5), 519-531. https://doi.org/10.1080/17445302.2018.1430200

Important note
To cite this publication, please use the final published version (if applicable).
Please check the document version above.

Copyright
Other than for strictly personal use, it is not permitted to download, forward or distribute the text or part of it, without the consent of the author(s) and/or copyright holder(s), unless the work is under an open content license such as Creative Commons.

Takedown policy
Please contact us and provide details if you believe this document breaches copyrights.
We will remove access to the work immediately and investigate your claim.

This work is downloaded from Delft University of Technology.
For technical reasons the number of authors shown on this cover page is limited to a maximum of 10.

Ships and Offshore Structures

ISSN: 1744-5302 (Print) 1754-212X (Online) Journal homepage: http://www.tandfonline.com/loi/tsos20

Numerical investigation of residual ultimate strength of dented metallic pipes subjected to pure bending

Jie Cai, Xiaoli Jiang & Gabriel Lodewijks

To cite this article: Jie Cai, Xiaoli Jiang & Gabriel Lodewijks (2018) Numerical investigation of residual ultimate strength of dented metallic pipes subjected to pure bending, Ships and Offshore Structures, 13:5, 519-531, DOI: 10.1080/17445302.2018.1430200

To link to this article: https://doi.org/10.1080/17445302.2018.1430200

© 2018 The Author(s). Published by Informa UK Limited, trading as Taylor & Francis Group

Published online: 01 Feb 2018.

Submit your article to this journal

Article views: 284

View Crossmark data

Full Terms & Conditions of access and use can be found at
http://www.tandfonline.com/action/journalInformation?journalCode=tsos20

SHIPS AND OFFSHORE STRUCTURES, 2018
VOL. 13, NO. 5, 519–531
https://doi.org/10.1080/17445302.2018.1430200

Taylor & Francis
Taylor & Francis Group

OPEN ACCESS Check for updates

Numerical investigation of residual ultimate strength of dented metallic pipes subjected to pure bending

Jie Cai [a], Xiaoli Jiang [a] and Gabriel Lodewijks [b]

[a]Department of Maritime and Transport Technology, Delft University of Technology, Delft, The Netherlands; [b]School of Aviation, University of New South Wales, Sydney, Australia

ABSTRACT

A dent is one of the main structural damages that may affect ultimate strength. In this paper, the residual ultimate strength of dented metallic pipes subjected to a bending moment is quantitatively investigated. The numerical model is developed accounting for the variation of the dent length (l_d), dent depth (d_d), dent width (w_d), dent rotation angle (θ_d) and dent location based on ABAQUS Python. The numerical model is validated by test results from a four-point bending test. Subsequently, a parametric investigation is performed on the effects of wave-type initial imperfection, D/t and dent geometrical parameters. It is found that both l_d and d_d have a significant effect on the residual ultimate strength of dented metallic pipes, while the effect of w_d is slight. Finally, an empirical formula with respect to l_d and d_d has been proposed for the prediction of bending moment, which can be deployed for practical purposes.

ARTICLE HISTORY
Received 17 May 2017
Accepted 12 January 2018

KEYWORDS
Residual ultimate strength; metallic pipe; dent; bending moment; empirical formula; nonlinear FEM

Nomenclature

κ	the curvature of pipe (1/m)
κ_0	the referential curvature of pipe (1/m)
κ_{cr}	the critical curvature of pipe (1/m)
λ_l	normalised dent length
λ_w	normalised dent width
λ_{cl}	critical half-wavelength
ω	dent depth variation (mm)
σ_u	material ultimate tensile strength (MPa)
σ_y	material yielding strength (MPa)
σ_{11}	stress component in pipe axial direction (MPa)
σ_{22}	stress component in pipe hoop direction (MPa)
σ_{eng}	engineering stress of material (MPa)
θ_d	dent angle (deg)
ε_0	referential strain of pipe
ε_{11}	strain component in pipe axial direction
ε_{22}	strain component in pipe hoop direction
ε_{eng}	engineering strain of material
D	outer diameter of pipe (mm)
d_d	dent depth (mm)
e_u	the maximum elongation of material
l'_d	dent length projected in pipe hoop direction (mm)
L_0	length of pipe under pure bending (mm)
l_d	dent length (mm)
M_i	ultimate bending moment of intact pipe (kNm)
M_y	plastic bending moment (kNm)
M_{cr}	residual ultimate bending moment (kNm)
n	material constant
R	pipe outer radius (mm)
t	pipe thickness (mm)
$U_{lateral}$	the maximum lateral displacement of pipe (mm)
w_d	dent width (mm)

1. Introduction

Structural damage in terms of a dent, metal loss and/or a crack on metallic pipes is unavoidable in engineering structures (Yang et al. 2007; Manes et al. 2012; Ghaednia et al. 2015; Zhang et al. 2015; Cai, Jiang, & Lodewijks 2017). The occurrence of damage could undermine structural integrity and strength, which may induce detrimental consequences. Meanwhile, with the widely applied limit state-based design (Paik and Thayamballi 2006; DNV 2013; Gong et al. 2013), every foreseeable failure scenario should be accounted for so that structures have sufficient load carrying capacity to afford potential structural damage. Hence, the residual ultimate strength of damaged structures should be carefully investigated. As one of the major structural damage, a dent could be introduced by accidental scenarios such as collision with foreign objects including rocks, anchors and fishing trawl boards (Park and Kyriakides 1996; DNV 2010). It is a permanent plastic deformation on a pipe wall that produces a gross distortion (Cosham and Hopkins 2004).

The past few decades have seen a considerable amount of research on residual ultimate strength of dented metallic pipes. Park and Kyriakides (1996) studied the collapse capacity of dented pipes under external pressure. The research found that the collapse capacity of pipes was relatively insensitive to the detailed geometry of a dent such as the shape and size, but was critically dependent on the maximum ovalisation of its most deformed cross-section. Orynyak et al. (1999) developed an ana-

CONTACT Jie Cai J.Cai-2@tudelft.nl

© 2018 The Author(s). Published by Informa UK Limited, trading as Taylor & Francis Group
This is an Open Access article distributed under the terms of the Creative Commons Attribution-NonCommercial-NoDerivatives License (http://creativecommons.org/licenses/by-nc-nd/4.0/), which permits non-commercial re-use, distribution, and reproduction in any medium, provided the original work is properly cited, and is not altered, transformed, or built upon in any way.

lytical equation to predict the bursting strength with respect to dimensionless length of dent ($\lambda_l = l'_d/\sqrt{Rt}$). Bjørnøy et al. (2000) investigated the bursting capacity of dented pipes subjected to internal pressure through experiments. A plain dent was introduced through a quasi-static indentation. Test results showed that significant reduction of the bursting capacity could be caused by a dent. When pipes are subjected to bending moment, Bai and Bai (2014b) proposed some empirical equations to predict the limit bending moment. Cai et al. (2016) numerically investigated dented pipes under dominant bending moment with axial force and internal pressure. Additionally, standards such as BSI (2005) and DNV (2013) have proposed relevant information for dented pipes to guide the design. Other relevant research on dents and other types of damage can also be seen from Macdonald and Cosham (2005), Gresnigt et al. (2007), Mohd et al. (2014), Ghaednia et al. (2015), Mohd et al. (2015), Lee et al. (2017), etc.

However, few fundamental research have been found on residual ultimate strength of dented pipes with D/t between 20 and 50 subjected to bending moment, which is a typical loading condition during pipe installation and operational phases (Kyriakides and Corona 2007). Simple formulas for prediction of the residual ultimate strength of dented pipes subjected to pure bending are still rare (Paik and Thayamballi 2006). The effects of dent parameters such as dent length (l_d) and dent depth (d_d) have not been quantitatively clarified. Based on the previous experimental research from the authors Cai, Jiang, Lodewijks, and Pei, et al. (2017), dented pipes with low D/t (around 21.3) have been studied. The aim of this paper is therefore to quantitatively investigate the residual ultimate strength of dented metallic pipes (D/t of 21.3) subjected to pure bending moment through nonlinear finite element method (FEM).

The structure of this paper is arranged as follows. In Section 2, geometric profile of dents is described in detail, while the finite element model is presented in Section 3. Then the model is validated based on tests in Section 4. The four-point bending test is first briefly reviewed, and the comparison results for dented specimens in terms of failure mode, strain distribution and bending-curvature diagram are presented. In Section 5, parametric investigation on the effects of initial imperfection, D/t, dent location and dent parameters on pipe strength is performed, and the corresponding strain distributions are presented. Based on these results, a prediction formula is proposed in Section 6. Finally, concluding remarks are made.

2. Damage description

A dent is a permanent plastic deformation on pipe wall that produces a gross distortion. In this paper, only a plain dent with a smooth curvature variation is accounted for, including the dent parameters in terms of dent length (l_d), dent width (w_d), dent depth (d_d), dent angle (θ_d) and dent location, as shown in Figure 1. The location of a dent is the centre of pipe cross-section on either the compression side or the tensile side of the pipe surface. The dent shape is postulated as a cosinusoidal shape, as expressed in Equation (1), where ω is the depth variation of the dent. In addition, the dent angle is defined as the angle between the dent axis in its length direction and the pipe axial direction, increasing along clockwise direction, as seen in Figure 1(b). Hence, a dent with the angle of 0° runs in the pipe's longitudinal direction. The l_d should be always larger than w_d in order to avoid ambiguity in this paper. In spite of the existing of impact induced residual stress around the dent region in practice, it has not been accounted for in this research due to the lack of test data. Based on the former research from the authors in Cai et al. (2016), its effect has been qualitatively investigated. Followed by a modelling of impact scenario between a pipe and a foreign object, residual ultimate strength of damaged pipes was then directly simulated through the import of residual stress. Only slight effect on pipe strength in terms of the bending moment has been observed.

$$\omega = d_d \cdot (1 + \cos(2\pi x/l_d)) \cdot (1 + \cos(2\pi y/w_d))/4 \qquad (1)$$

There are two aspects that determine the selection of the dent size in this paper: On the one hand, a tiny dent could be considered as the initial imperfection. On the other hand, an extra large dent may induce sudden collapse of the structure, which is meaningless to take into account. Hence, the selected d_d/t in the

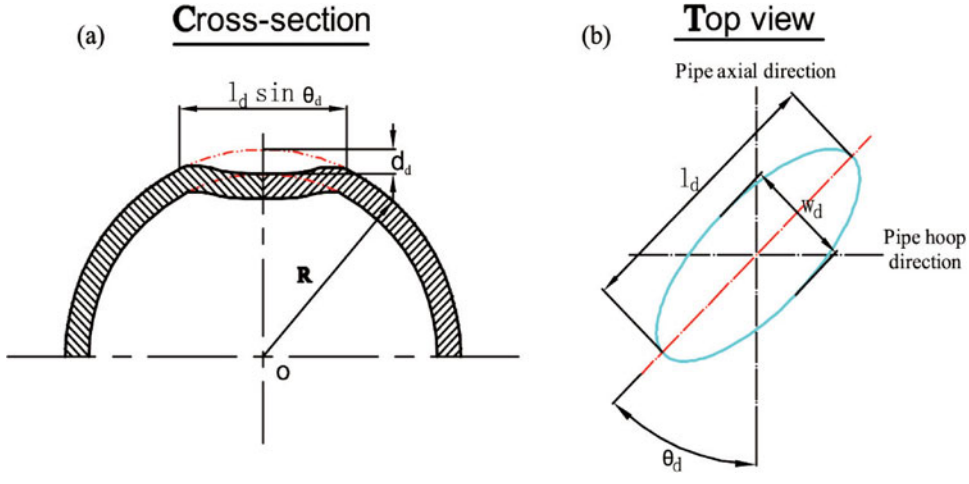

Figure 1. Sketch of a plain dent on pipe surface: (a) dent cross-section; (b) top view. (This figure is available in colour online.)

Table 1. Principal dimension of pipe models for simulation.

Pipe type	Diameter D (mm)	Thickness t (mm)	Length L_0(mm)	D/t	L_0/D	Material
Seamless	168.3	7.9	720	21.3	4.28	Q345 (GB/T 1591 2008)

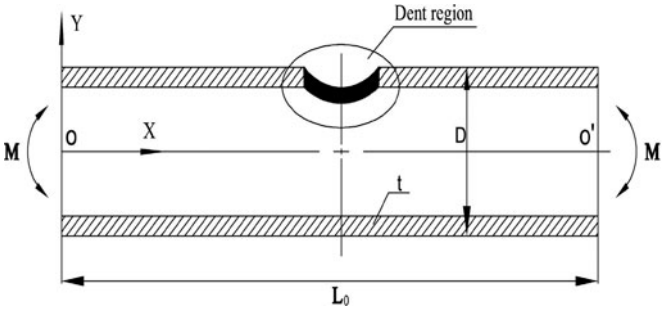

Figure 2. Sketch of dented pipe subjected to pure bending moment.

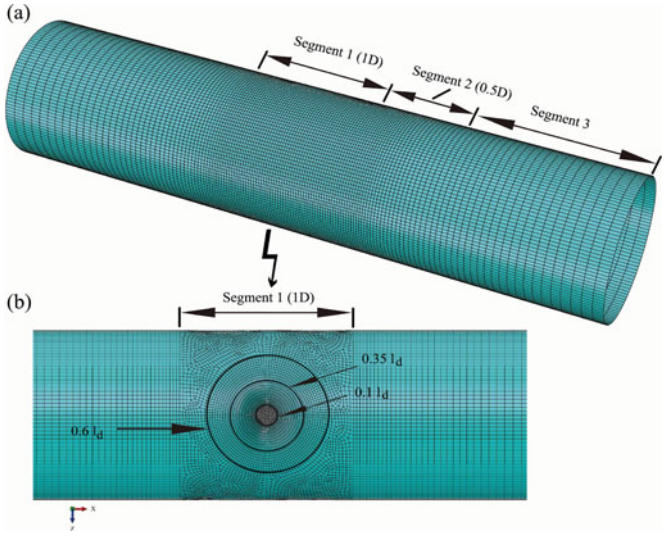

Figure 3. FEA model of dented pipe: (a) general mesh distribution; (b) refined dent region. (This figure is available in colour online.)

following research is between 0.13 and 2.0, and the normalised dent length $l'_d/\sqrt{Rt}$ is between 0.4 and 5.0.

3. Finite element model

A numerical model of a pipe with dent (Figures 2 and 3) is developed in ABAQUS/Standard (Abaqus6.13 2013) through python for the simulation of dented pipes, accounting for the varying of dent length (l_d), dent depth (d_d), dent width (w_d), dent rotation angle (θ_d) and dent location. Some simplifications have been made in this model compared with the test configuration (description in Section 4). For instance, only the pipe segment under pure bending is accounted for. Two reference nodes (O and O') coupled with the respective pipe end cross-section have been introduced to represent the loading locations, exerting an equivalent forced-rotation with a uniform angle of 0.001 in every increment. In this way, a uniform bending moment is introduced, which can produce the same loading procedure as the four-point bending test. The dent is put on the central cross-section of pipes.

A simply supported boundary condition is deployed in this model. Rotations along X and Y axis at both pipe ends are restricted so that no torsion would be induced during simulation. All the translations are restricted in the pipe end O (Figure 2), while the axial translation is set to free in the other end O' so that no extra axial force would be induced. The symmetry of model has not been introduced due to the occurrence of dent. The principal dimensions of pipe model for the following parameter studies are summarised in Table 1. Initial imperfection in terms of a wave-type (wrinkling) is accounted for in this model based on a similar pipe research by Es et al. (2016) and Vasilikis et al. (2015). The imperfection is obtained from a standard eigenvalue simulation of a pipe, in the form of its first-order buckling mode with an amplitude of $0.01t$ (typical value from 0.01t to 0.12t as reported in Es et al. 2016).

The cylindrical shell is modelled with a curved three-dimensional shell element (S8R5), which is an 8-node, quadrilateral element with reduced integration and five degrees of freedom in each node (three displacement components and two in-surface rotation components), providing an accurate and economical simulation. The mesh strategy of the finite element analysis (FEA) model is shown in Figure 3, partitioning the entire model into three different segments. The length of central segment (segment 1) is set to $1D$ (D is outer diameter of pipe) with the maximum element size of 3 and 4 mm in pipe longitudinal and hoop direction, respectively, i.e. less than 9% of the critical half-wave length ($\lambda_{cl} = 1.728\sqrt{Rt}$ (Prabu et al. 2010)). Segment 2 is a mesh transition region with a length of $0.5D$, arranging with a biased mesh, while segment 3 has a coarse distribution of mesh with the maximum element size of 12 mm.

In the damaged region, as illustrated in the zooming in region in Figure 3(b), mesh is largely refined. The geometry of this region is further partitioned into three concentric circular regions, with the radius of $0.1l_d$, $0.35l_d$, and $0.6l_d$, respectively. The aim of such mesh strategy is to fashion a well-organised mesh distribution so that the possible artificial local bending stress and stress concentration would be avoided. The maximum mesh size of inner circle is strictly limited within 2 mm with a structured mesh strategy, i.e. less than 4% of one half-wave length λ_{cl} of cylindrical shells. The maximum mesh size of outer regions is limited within 3 mm with a sweep mesh strategy, i.e. more than 14 elements in one critical-half wavelength.

3.1. Material properties

A typical pipe material Q345B (GB/T 1591 2008) is deployed, which is a type of pipe structural steel with high strength and large ductility. An elastic–plastic property with Von Mises yielding criterion and isotropic hardening is deployed. The strain-hardening effect of material is developed by the Ramberg–Osgood equation (Ramberg and Osgood 1943) based on measured material parameters from the test, as seen in Equation (2). Where n is the material constant, ε_{eng} and σ_{eng} are the

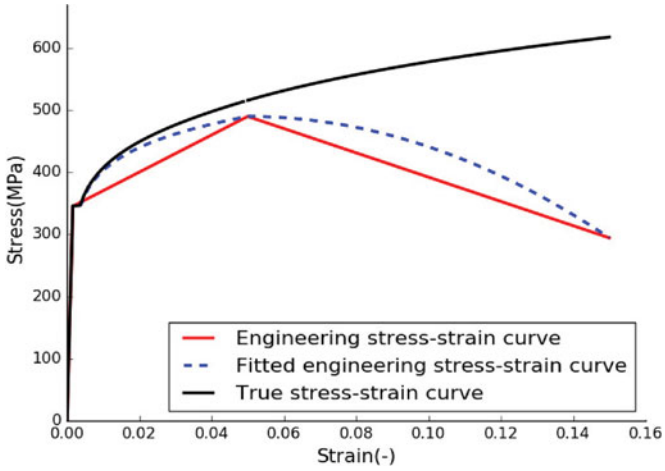

Figure 4. The fitted true stress-strain curve for numerical investigation. (This figure is available in colour online.)

engineering strain and stress, respectively. It should be noted that an assumption of 0.002 plastic strain for ductile material at yielding point is made in this equation.

$$\varepsilon_{\text{eng}} = \sigma_{\text{eng}}/E + 0.002(\sigma_{\text{eng}}/\sigma_y)^n \tag{2}$$

The true stress–strain curve used in the numerical simulation is shown in Figure 4, which is fitted through basic material properties including the material yielding strength σ_y, ultimate tensile strength σ_u and the maximum elongation e_u with an assumption that σ_y, σ_u and material failure happen on the strain of 0.002, $e_u/3$ and e_u, respectively (Pakiding 2007; Cai et al. 2016). In the following research of dent parameters in Section 5, the σ_y, σ_u and e_u are assumed as 345 MPa, 490 MPa and 0.15 (except the model validation by test in Section 4), respectively.

4. Model validation

In this section, simulations for test specimens are carried out based on the developed numerical model in the previous section. The prediction model has been validated through the comparison between numerical results and test data.

4.1. Reference values

Generally, bending moment is normalised by the plastic bending moment $M_y = 4R^2t\sigma_y$, while the curvature κ is normalised by a curvature-like expression $\kappa_0 = t/4R^2$. Only global curvature is used for comparison afterwards between the test and numerical simulation. The selected locations for calculation of global curvature in simulation are exactly the same with tests, while the bending moment is the resultant of all the node forces multiplying their corresponding force arms in the central cross-section of specimen in simulation. The bending moment M_i from intact pipe is used as the reference value for the proposed formula in Section 6.

4.2. Test description

In order to investigate the residual ultimate strength of damaged pipes, a four-point bending test has been successfully designed and carried out. The configuration of test set-up is presented in Figure 5, which consists of different structural segments. The

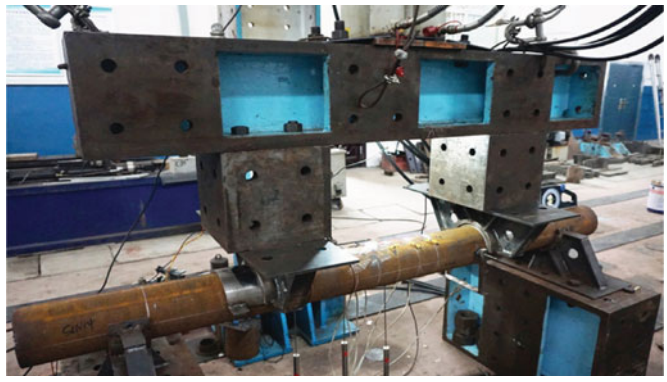

Figure 5. Configuration of four-point bending test set-up in laboratory. (This figure is available in colour online.)

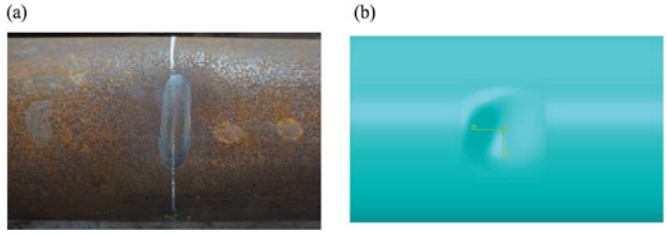

Figure 6. Dent damage from both test and numerical models: (a) artificial dent damage on specimen; (b) dent damage on numerical model. (This figure is available in colour online.)

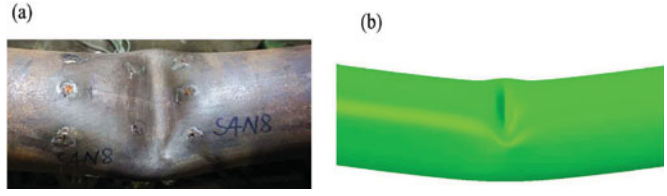

Figure 7. Comparison of failure mode between test and simulation (S2N1). (This figure is available in colour online.)

overall length of the specimen is 2200 mm with the length of 800 mm under pure bending. The test results were measured and documented extensively. The structural damage was introduced properly on each specimen before the strength test, locating at the centre of specimen either on the compression side or on the tensile side. Different types of indentors were designed and fabricated to produce dents with varied shape. Through a quasi-static indentation, the dent was then introduced on the specimens with different rotation angle such as 90°, 45° and 0°. Figure 6 shows the introduced dent damage from both test and the corresponding numerical models, while Table 2 lists the detailed information of the dented specimens.

It should be noted that the developed numerical model in this paper is not exactly the same as the real test configuration, but is simplified in a reasonable way. For instance, the model has been simplified by only keeping the pure bending segment. An equivalent simply supported boundary condition is used to represent the real boundary, ignoring the real frictions between specimen and loading strips. A displacement-control loading strategy is employed instead of the load-control strategy in the test. The material that deployed is type 'L7' from the test.

Table 2. Summary of both test and simulation results on dented specimens (dimension unit: mm; angle unit: degree; dents are on the compression side of specimens).

S.N.	D	t	D/t	Dent ($l_d \times w_d \times d_d$)	Dent angle	BM (test) (kNm)	BM (FEA) (kNm)	Discrepancy (%)	κ (test) (1/m)	κ (FEA) (1/m)	Discrepancy (%)
S2N1	169.21	8.25	20.51	89 × 68 × 10.3	90	92.57	91.75	− 0.89%	0.154	0.124	− 19.48%
S2N2	168.23	8.13	20.69	100 × 75 × 10.3	90	93.55	87.53	− 6.44%	0.109	0.108	− 0.92%
S2N3	169.38	7.90	21.44	130 × 60 × 10.3	45	91.65	92.25	0.66%	0.158	0.122	− 22.79%
S2N5	168.74	8.15	20.70	110 × 85 × 10.3	90	90.97	87.00	− 4.36%	0.164	0.101	− 38.42%

4.2.1. Structural failure mode

The comparison of structural failure modes is illustrated in Figure 7. The result shows that a similar failure mode from simulation has been induced in the local dented region. As a result of the increase of structural deformation in the form of ovalisation in pipe cross-sections, the specimen subjected to increasing bending moment fails. Under certain extent, such ovalisation can be counterbalanced by material yielding and further hardening of material so that structure keeps stable. When the ovalisation cannot be compensated for, the structure reaches its bending capacity with the largest ovalisation in a specific pipe cross-section. For the pipe with a dent, the failure initiates and propagates in the dent region in the form of an inward bulge.

The failure of the structure is also reflected by the variation of strain, as illustrated in Figure 8. The test results from the

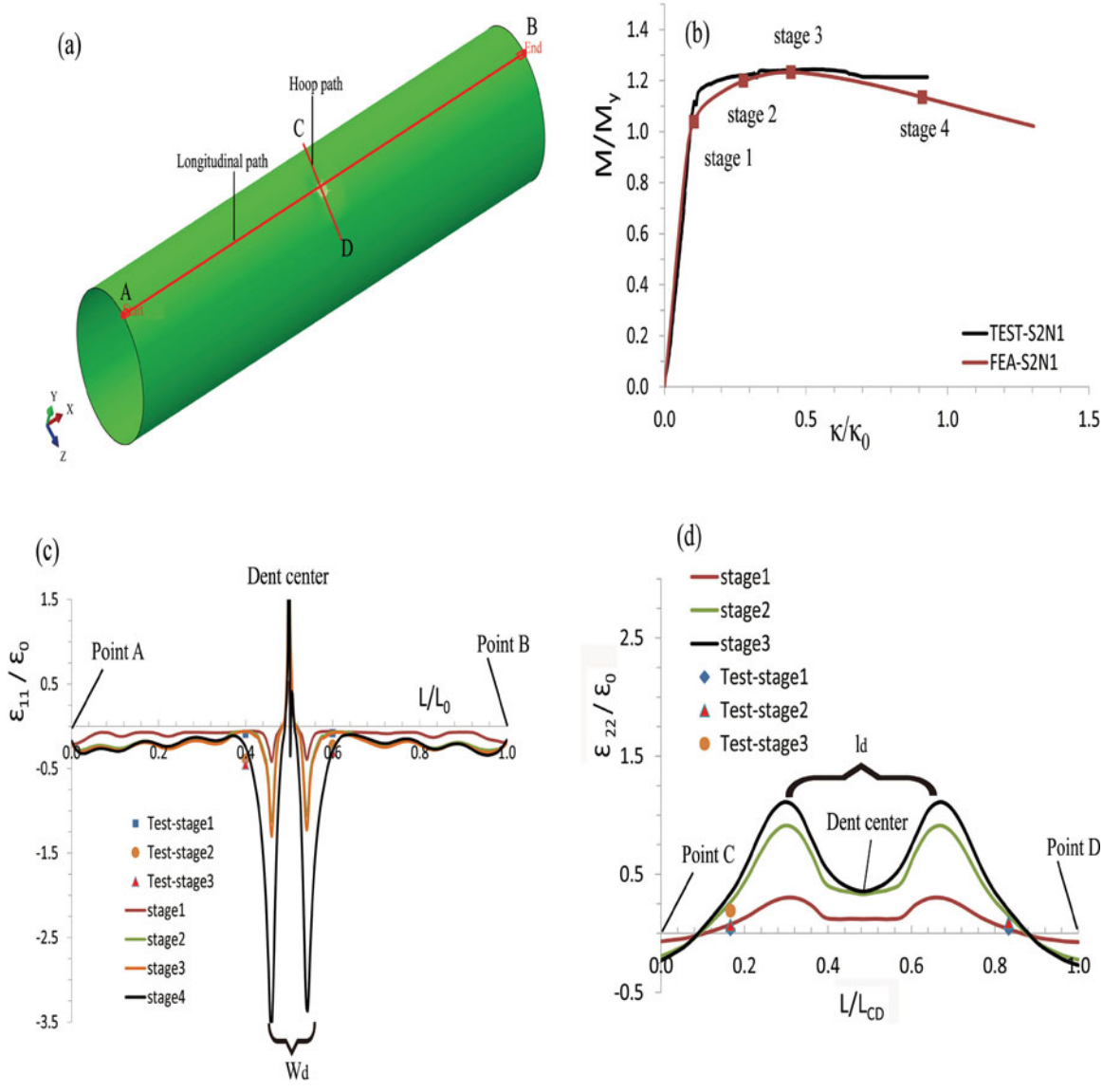

Figure 8. (a) Sketch of representative paths on specimen surface (S2N1); (b) four stages during the loading procedure; (c) strain along the longitudinal path AB; (d) strain along the hoop path CD. (This figure is available in colour online.)

measurement of strain gauges in specific points and corresponding stages are presented. It shows the evolution of both axial strain (ε_{11}) and hoop strain (ε_{22}) along the pipe longitudinal path and the hoop path across the dent centre (the chord length of CD is 120 mm), respectively. The strain here is normalised by ε_0, which can be expressed as $\varepsilon_0 = \kappa_0 D/2$. It is observed that the occurrence of a dent has changed the strain distribution from the beginning stage, and a localisation of strain happens in the dented region, concentrating on both the dent centre and the dent edge (Figure 8(c,d)).

Most of the strains measured from test lie on or close to the prediction curves. However, discrepancy exists due to the limit measurement range of stain gauges (±3%), workmanship of gauge and the possible effect of shear force that was introduced by loading heads. For the hoop strain ε_{22}, as shown in Figure 8(d), it starts with a small compression value on point *C* in the beginning stage outside the dent region, and then turns to a large tensile value inside the dent region, decreasing all the way to the dent centre. This phenomenon implies the fashion of the inward bulge and the increasing tendency of the ovalisation in the dented cross-section.

4.2.2. Moment-curvature diagrams

The representative bending moment-curvature diagrams for the comparison between test data and numerical prediction are presented in Figure 9. Table 2 lists all the comparison results in terms of bending moment and critical curvature. Three specimens (S2N1, S2N2 and S2N5) contain dent in 90° on the compression side, while the specimen S2N3 contains dent in 45° on the compression side.

The diagrams show a satisfying prediction from the numerical simulations in terms of failure tendency and maximum bending moment, i.e. less than 6.5% discrepancy compared with the test. A relatively large scatter occurs on the critical curvature, i.e. the largest discrepancy of −38.42% in specimen S2N5. However, the prediction for curvature is conservative, which is due to the ignorance of frictions of test configuration in the simplified boundary condition of numerical model used in this paper. Moreover, factors such as material properties, as discussed in the experimental investigation (Cai, Jiang, Lodewijks, & Pei, et al. 2017), are also related to the discrepancies. Accounting for these reasons, it is safe to conclude that the developed simplified numerical model is capable of predicting the bending behaviour of pipes with a conservative prediction.

Additionally, both numerical predictions and test data indicate that the elastic–plastic failure pattern is dominant with a relative smooth failure of specimen, and significant plastic effect happens with the bending capacity (M_{cr}) exceeding plastic bending moment M_y. For the damaged specimen, M_{cr} is more than 1.12 times of M_y based on the simulation predictions. The occurrence of a dent has changed the variation tendency of bending moment-curvature diagrams, initiating a rapid

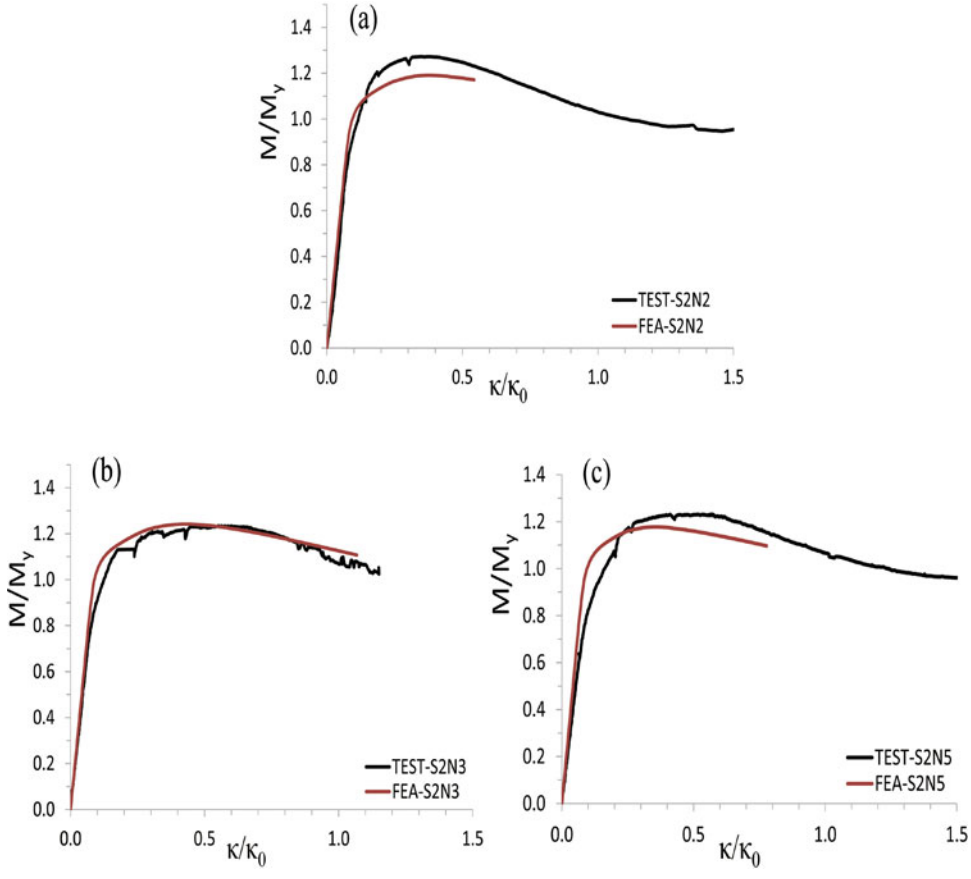

Figure 9. Comparison between numerical and test results in terms of bending moment-curvature diagram for specimens with dent: (a) specimen S2N2 with 90° dent on compression side; (b) specimen S2N3 with 45° dent on compression side; (c) specimen S2N5 with 90° dent on compression side. (This figure is available in colour online.)

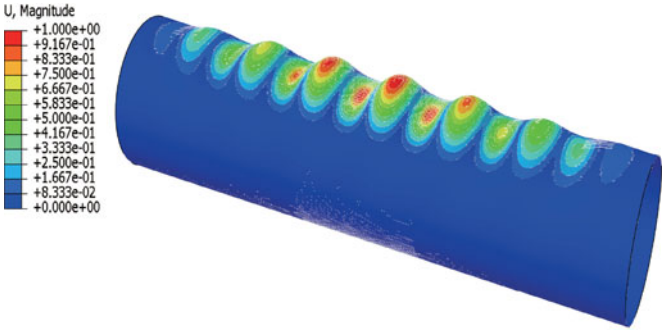

Figure 10. The first eigenvalue-buckling mode of a perfect pipe subjected to pure bending. (This figure is available in colour online.)

failure of specimen and considerably reducing the critical bending curvature.

5. Parametric investigation

Through the validated numerical model, different parameters of pipes will be investigated in the present section. Specifically, the effects of diameter-to-thickness ratio (D/t), dent location, dent angle (θ_d), dent length (l_d), dent depth (d_d) and dent width (w_d) are investigated. Numerical results in terms of residual ultimate bending moment (M_{cr}), critical curvature (κ_{cr}), lateral displacement ($U_{lateral}$) and stress distribution are presented and discussed. The principal dimensions of pipe model are summarised in Table 1.

5.1. Initial imperfection

In practice, the initial imperfection on pipe structures in terms of ovalisation or wrinkling exists due to constructions, external water, bending moment or other relevant causes. From the standpoint of the pipe design, the minimum value of 0.5% for pipe ovalisation is used in DNV (2013). However, the initial imperfections normally allowed in pipeline design do not significantly influence the moment capacity under pure bending (Hilberink 2011; Bai and Bai 2014a), especially for the seamless pipes with lower D/t. Hence, the simulation results on the damaged pipes would not be affected by neglecting such imperfection.

In spite of the insignificant effect, an investigation of the initial imperfection in terms of wrinkling is still conducted. Hence, five different amplitudes, varying among $0.1t$, $0.05t$, $0.02t$, $0.01t$ and $0.001t$, are deployed, while the specific shape of imperfection is in the form of the first-order of the eigenvalue buckling modes, as illustrated in Figure 10.

Figure 11 shows the bending moment-curvature diagram with varying of initial imperfections for an intact pipe without damage. Results indicate that both the bending moment and corresponding critical curvature vary with the variation of initial imperfection, decreasing with the increase of imperfection amplitude. The occurrence of the initial imperfection can accelerate the failure of the structure. The effect on critical curvature is slight when the wrinkling amplitude is no larger than $0.02t$. However, only a slight effect on the bending moment has occurred, which demonstrates the former statement.

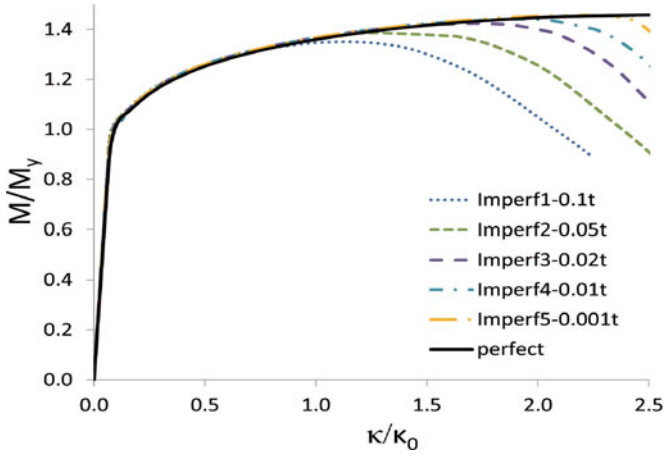

Figure 11. Bending moment-curvature diagram of a pipe with varying of initial imperfection (no dent damage). (This figure is available in colour online.)

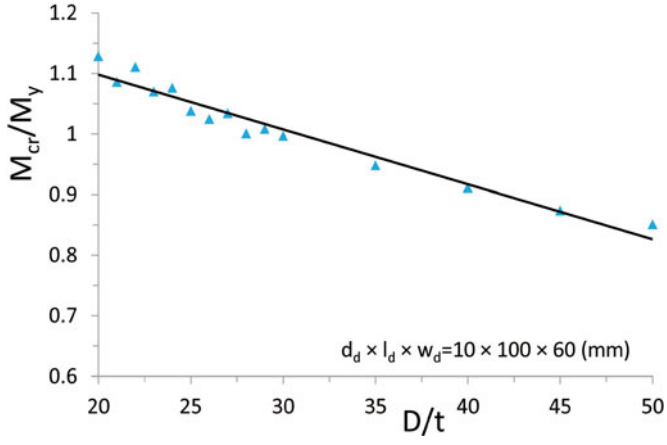

Figure 12. The bending capacity of a dented pipe with varying of D/t. (This figure is available in colour online.)

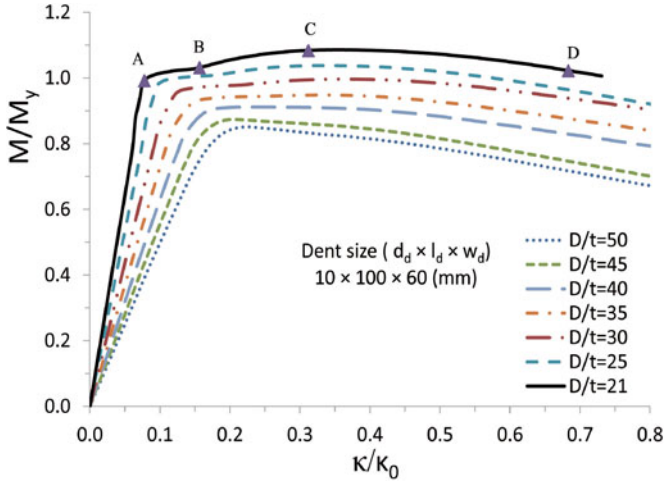

Figure 13. Bending moment-curvature diagram with varied diameter-to-thickness ratio (D/t). (This figure is available in colour online.)

5.2. Effect of diameter-to-thickness ratio (D/t)

As one of the critical parameters, the pipe diameter-to-thickness ratio (D/t) affects the residual ultimate strength and corresponding failure mode of metallic pipes. With the decrease of the D/t ratio, the failure mode of structures will gradually change from

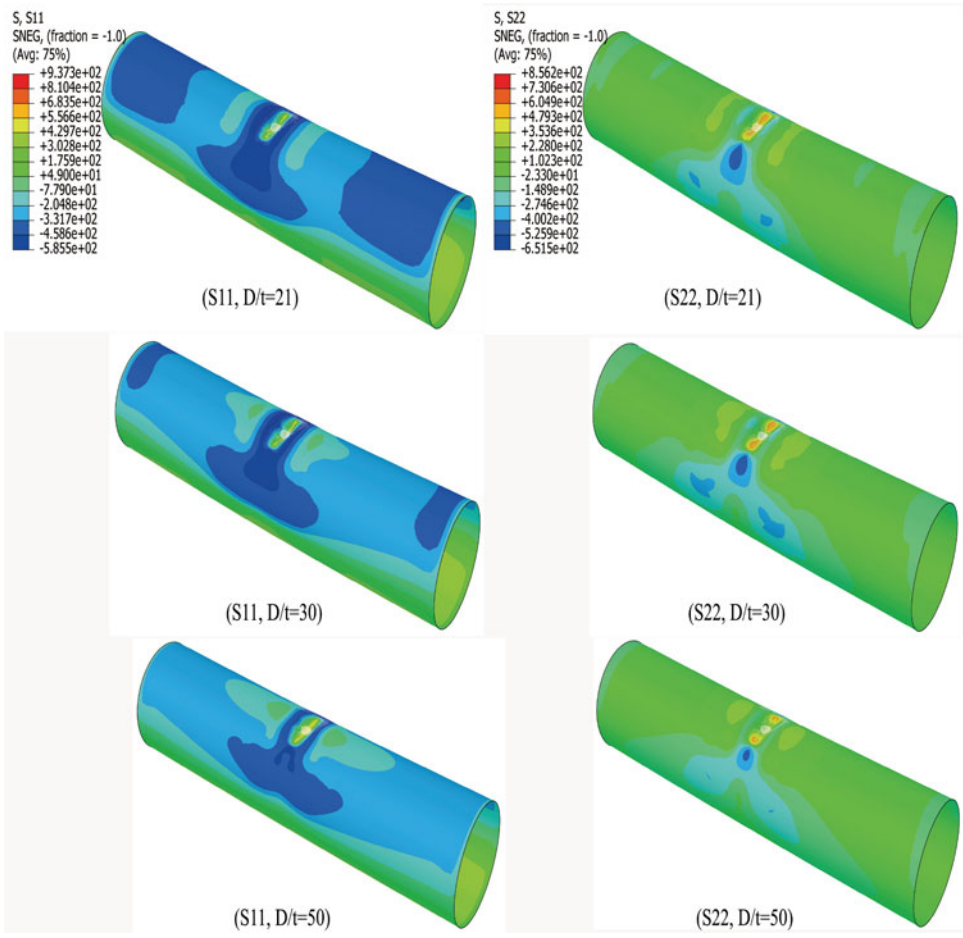

Figure 14. Membrane stress distribution of a dented pipe with different diameter-to-thickness ratio at the ultimate bending point. (This figure is available in colour online.)

an elastic buckling to an elastic–plastic buckling or even fracture failure. Figure 12 presents the variation of normalised bending capacity with respect to D/t between 20 and 50. A plain dent is postulated in the pipe centre on the compression side of the pipe surface. All the dent angles are set to 90° (the pipe hoop direction). It is found that, with the increase of the D/t, the residual strength of a dented pipe decreases approximately in a linear way.

Figure 13 denotes the normalised bending moment-curvature diagram of dented pipes with varying of D/t ratio. The curvatures here are calculated from the longitudinal strain (ε_{11}) on the bottom of pipe central cross-section ($\kappa = 2\varepsilon_{11}/D$). It implies that different failure modes have happened, for instance, for a pipe with D/t of 21, the elastic–plastic failure happens with $M_{cr} = 1.09M_y$, whereas for pipe with $D/t = 50$, elastic buckling happens with a small ultimate bending moment, equal to $0.77M_y$. The structure fails smoothly with the increase of bending moment for pipes with $D/t = 21$. Structure first reaches the linear limit point, as seen from Point A. Then, the plastic deformation starts to occur and expanding until Point B due to the material hardening effect. When the bending energy is keeping accumulation, the limit point C has been reached. Afterwards, the strength capacity of pipes does not increase anymore, but gradually decreases with the rapid increase of plastic deformation until the critical collapse point D has been reached. In contrast, for pipes with large D/t, a sudden collapse happens once the limit point has been reached, as seen in the dotted curve of $D/t = 50$.

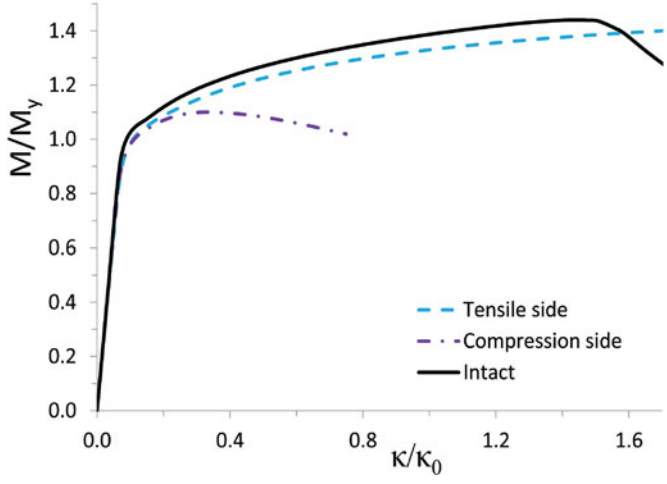

Figure 15. Bending moment-curvature diagram of pipes with varying of the dent location ($l_d = 100$ mm, $w_d = 60$ mm). (This figure is available in colour online.)

Figure 14 shows the membrane stress distribution of a dented pipe with different D/t including 21, 30 and 50 at the ultimate bending point. σ_{11} and σ_{22} are the stress components in the

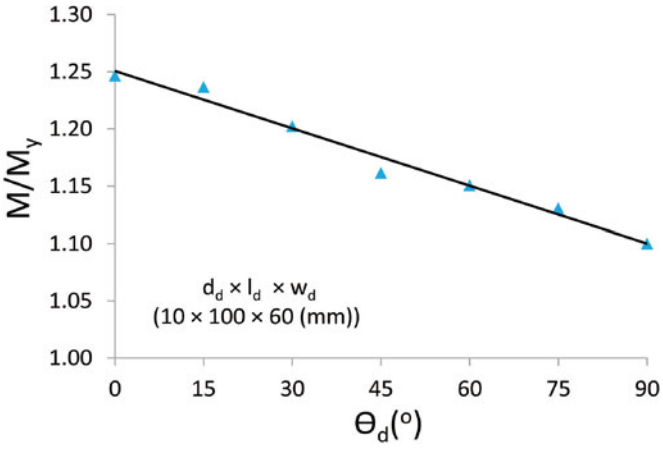

Figure 16. The bending capacity of a dented pipe with varying of dent rotation angle. (This figure is available in colour online.)

pipe axial direction and hoop direction, respectively. It is found that the stress distribution has been largely changed due to the occurrence of dent damage. It is also observed that a high compression stress region occurs at the dent tip, while a low tensile stress region occurs adjacent to the dent in the pipe longitudinal direction. With the decrease of the D/t ratio, such high stress region is prone to increase, whereas the low stress region is prone to concentrate. The overall plastic region at the ultimate bending point with small D/t is much larger than the one with large D/t.

5.3. Effect of dent location

Figure 15 is the normalised bending moment-curvature diagram of pipes with varying of the dent location. The dent angle is set to 90° (pipe hoop direction) with a dent length of 100 mm and a width of 60 mm. It is found that a dent on the compression side has produced a significant negative effect on structure strength in terms of the maximum bending moment and critical curvature, whereas a dent on the tensile side only has a slight negative effect on the bending moment compared with the intact case. The critical curvature has been enlarged due to the recovery of the dent on the tensile side, which conforms to the observation in test. However, it should be noted that the fracture failure has not been accounted for in this paper, which may dominate the behavior of pipes with a dent on their tensile side.

5.4. Effect of dent orientation

The dent orientation also affects the load carrying capacity of damaged pipes. Figure 16 shows the diagram with respect to the critical bending moment and dent angle. A moderate dent ($d_d \times l_d \times w_d = 10 \times 100 \times 60$ mm) is postulated in pipe

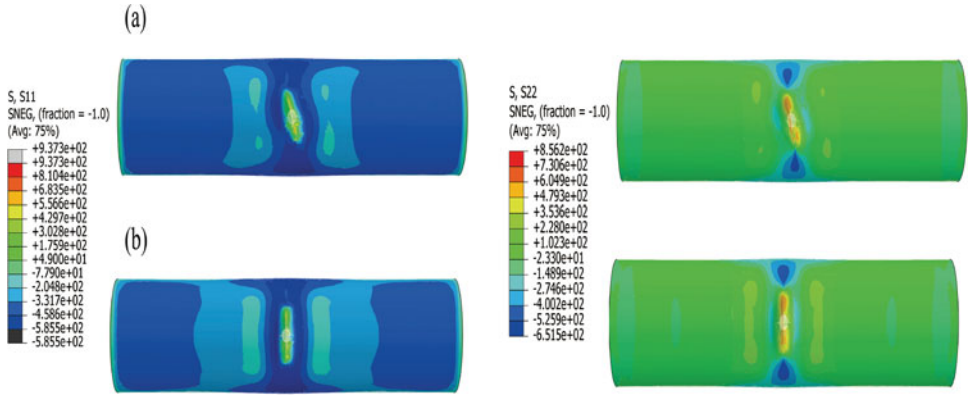

Figure 17. (a) Membrane stress distribution of a dented pipe with dent rotation angle $\theta_d = 45°$ at the ultimate bending point; (b) membrane stress distribution of a dented pipe with dent rotation angle $\theta_d = 90°$ at the ultimate bending point. (This figure is available in color online.)

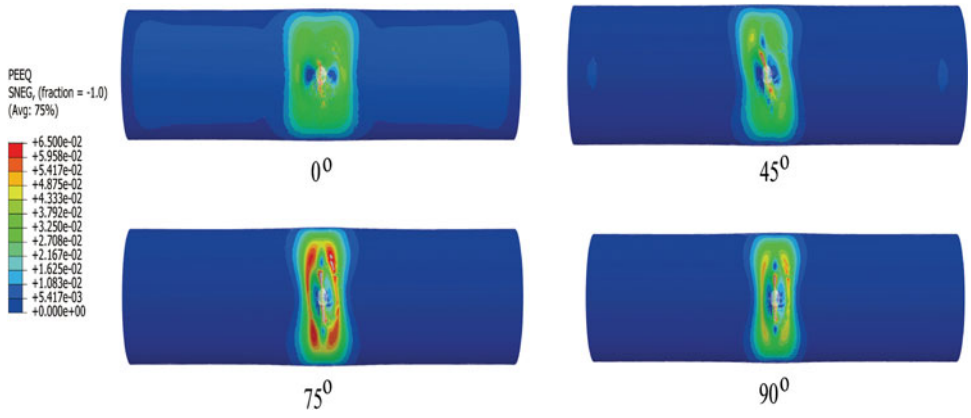

Figure 18. Equivalent plastic strain (PEEQ) of a dented pipe with varying of dent rotation angle (θ_d) at the ultimate bending point. (This figure is available in color online.)

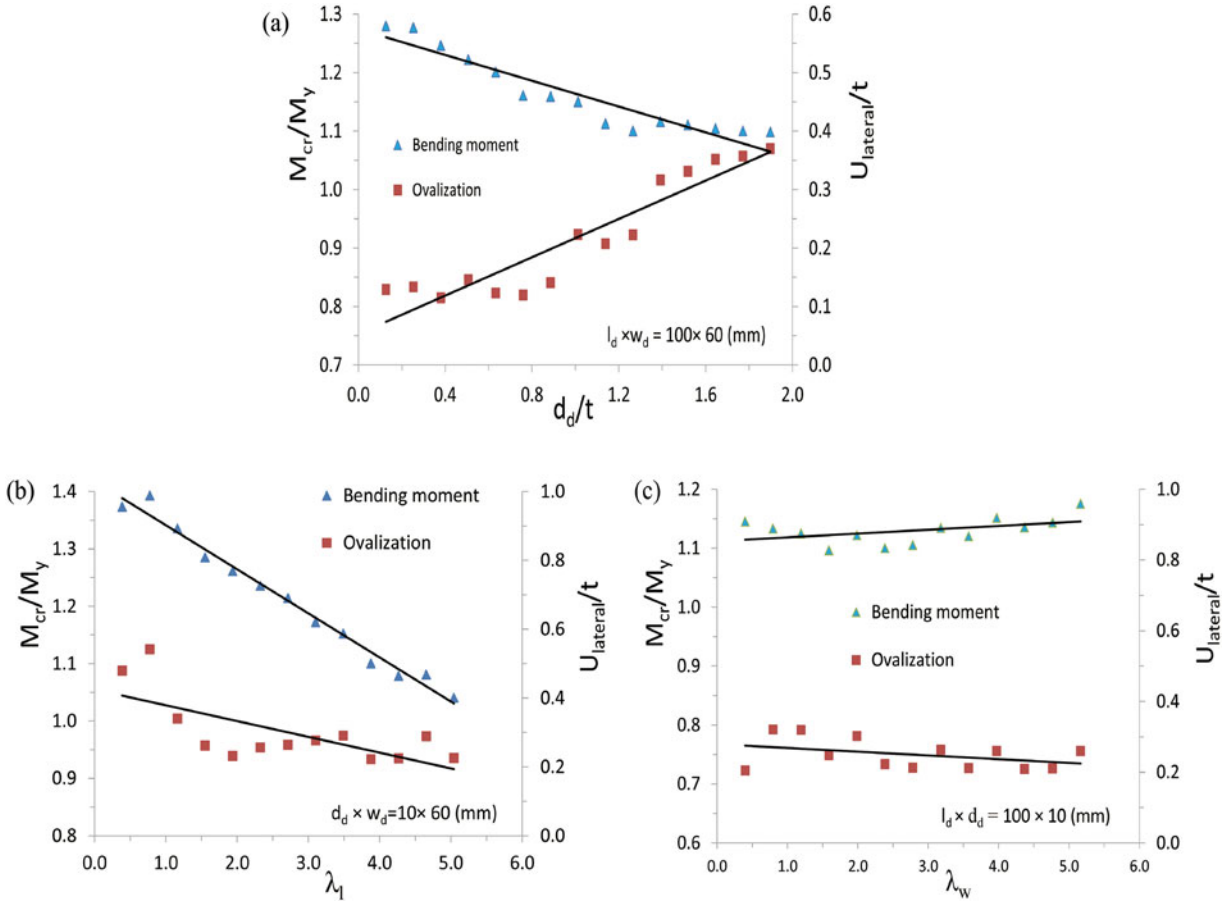

Figure 19. The structural response in terms of bending capacity and maximum lateral displacement of pipe with varying of different parameters: (a) dented pipe with varying of dent depth; (b) dented pipe with varying of dent length; (c) dented pipe with varying of dent width. (This figure is available in colour online.)

surface on the compression side. As demonstrated by the simulation results, the larger the dent rotation angle (θ_d) is, the smaller the residual ultimate strength will be. In other words, a pipe with a hoop dent on its compression side is the most critical condition for the bending capacity.

Figure 17 shows the membrane stress distribution of a dented pipe with the varying of the dent rotation angle. Only two angles are presented for clarity reason. The highest stress happens inside the dent. There is a low compression stress region in terms of σ_{11} along the pipe longitudinal direction, whereas a large tensile stress in terms of σ_{22} occurs at the dent tips. With the increase of the dent rotation angle, the compression region is increasing and the distributions of both stress components become uniform.

Figure 18 illustrates the variation of the equivalent plastic strain (PEEQ) region of a dented pipe with varied θ_d at the ultimate limit point. The PEEQ, as a function of the plastic strain, is a scalar measurement of the accumulated plastic strain, which

Table 3. Residual ultimate strength of pipes with varying of dent depth.

	$l'_d = 100$ mm, $w_d = 60$ mm d_d/t											
Capacity	0.13	0.25	0.38	0.51	0.76	1.01	1.27	0.1.39	1.52	1.65	1.77	1.90
M_{cr}/M_y	1.279	1.277	1.246	1.222	1.161	1.150	1.100	1.10	1.110	1.104	1.100	1.098
$U_{lateral}/t$	0.13	0.13	0.11	0.15	0.12	0.22	0.22	0.33	0.33	0.35	0.36	0.37

Table 4. Residual ultimate strength of pipes with varying of dent length.

	$d_d = 10$ mm, $w_d = 60$ mm $\lambda_l = l'_d/\sqrt{Rt}$											
Capacity	0.389	0.776	1.164	1.551	1.939	2.327	2.715	3.103	3.491	3.878	4.266	5.042
M_{cr}/M_y	1.374	1.393	1.335	1.285	1.261	1.236	1.214	1.172	1.152	1.100	1.078	1.040
$U_{lateral}/t$	0.48	0.54	0.34	0.26	0.23	0.26	0.26	0.28	0.29	0.22	0.22	0.23

Table 5. Residual ultimate strength of pipes with varying of dent width.

	$d_d = 10$ mm, $l'_d = 100$ mm $\lambda_w = w_d/\sqrt{Rt}$											
Capacity	0.397	0.795	1.192	1.589	1.986	2.384	2.781	3.178	3.576	3.973	4.370	5.165
M_{cr}/M_y	1.145	1.133	1.125	1.096	1.122	1.100	1.105	1.134	1.120	1.151	1.135	1.175
$U_{lateral}/t$	0.20	0.32	0.32	0.25	0.30	0.22	0.21	0.26	0.21	0.26	0.21	0.26

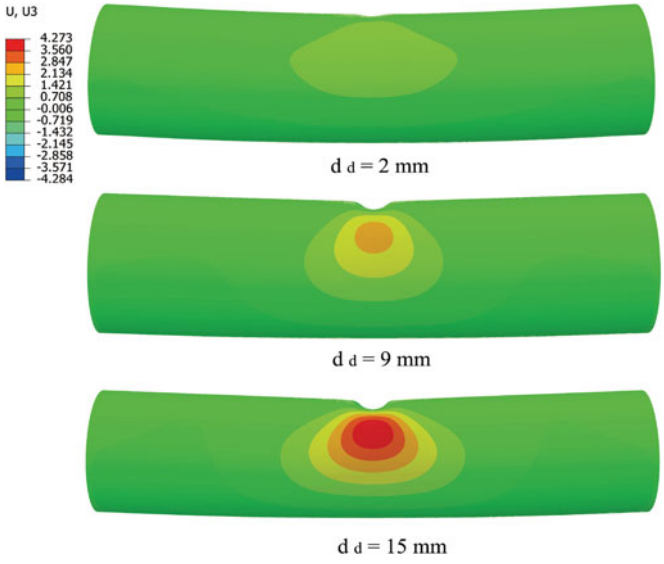

Figure 20. Lateral displacement distribution of a dented pipe with the varied dent depth d_d at the residual limit point. (This figure is available in color online.)

is equivalent to the Mises stress. The range of the legend for PEEQ here is between 0% and 6.5%. It is found that, with the increase of dent angle, the plastic region gradually concentrates, fashioning four regular lobes adjacent to the dent. Structure fails as a consequence of the extra large and concentrated plastic strain.

5.5. Effect of dent depth

By changing the dent parameters, a series of numerical simulations on dented pipes are carried out to identify their effects. The simulation results are presented in Tables 3–5. As shown in Figure 19(a), the residual strength decreases rapidly with the increase of d_d/t, and the ovalisation in terms of the largest lateral displacement has an increasing tendency with the increase of d_d/t. It can be also seen in Figure 20 that, the larger the dent depth, the larger the ovalisation will be. For instance, the lateral displacement reaches the largest value 4.273 mm at the strength limit point at $d_d = 15$ mm. In contrast, the lateral displacement is only 1.38 mm at $d_d = 2$ mm. It is also observed that, with the increase of the dent depth, the location with the largest lateral displacement is gradually moving to the dent tip region.

5.6. Effect of dent length

The dent length significantly influences the pipe residual strength, as shown in Figure 19(b). The bending capacity decreases with the increase of dent length. Meanwhile, the ovalisation capacity in terms of the largest lateral displacement in the central cross-section of pipe decreases from $0.5t$ to $0.2t$ with the increase of l_d, and keeps nearly stable when the dent dimensionless length ($l_d/\sqrt{Rt}$) is larger than 0.3.

5.7. Effect of dent width

The dent width in the pipe longitudinal direction has an insignificant effect on the pipe residual strength subjected to pure bending. Figure 19(c) shows the effect of dent width and the corresponding largest lateral displacement in the central dented cross-section with the varying of w_d. It is obvious that the strength capacity only has a slight variation in each case.

6. Prediction equations

As discussed in the previous section, the dent length and dent depth are two critical parameters that affect the residual ultimate strength of a dented metallic pipe subjected to pure bending. Due to the insignificant effect of the dent width, it has not been taken into account in the proposed equation. Hence, it is reasonable to construct an empirical equation in the function of $l'_d/\sqrt{Rt}$ and d_d/t, as expressed in the following equation:

$$M_{cr}/M_i = 1 - f(d_d/t, l'_d/\sqrt{Rt}) \tag{3}$$

where l'_d is the projected length of the dent in the pipe hoop direction in order to account for the effect of dent angle ($l'_d = l_d \sin\theta_d$, $\theta_d \in (0, 90]$).

A regression analysis is carried out based on the FEM results. The fitted coefficients for residual bending moment are obtained as a consequence.

$$M_{cr}/M_i = 1 - \eta(d_d/t)^{a_1}(l'_d/\sqrt{Rt})^{a_2} \tag{4}$$

Where η, a_1 and a_2 are 0.076, 0.346 and 0.716, respectively. Analysis of variance (ANOVA) shows that the R square of the proposed formula is 0.935, which indicates that it has a satisfying fit.

Figure 21 explicitly presents the prediction accuracy of the formula based on the comparison to the test and numerical results. As seen in Figure 21(a), a good correlation is obtained between empirical prediction and FEM, where the abscissa denotes the normalised proposed results from Equation (4), the ordinate denotes the normalised results from both FEM and test. Here, the M_i for the test is from specimen S1N4 (M_i = 102.71 MPa), while it is 101.014 MPa from an intact pipe based on numerical simulation. Compared to the test data, the formula provides a conservative prediction. Moreover, a diagram of prediction by using the formula is presented with the variation

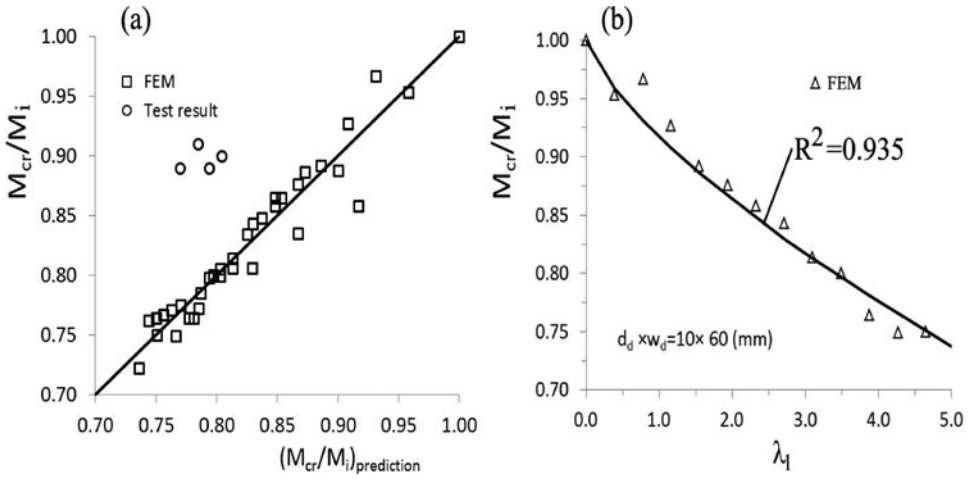

Figure 21. Comparison of model accuracy: (a) comparison between predictions and both test and simulation results (M_{cr}/M_i); (b) prediction of strength with varying of dent parameter (λ_l).

of dent length (λ_l), as seen in Figure 21(b). A high agreement between each other can be seen.

Practically, the proposed formula can be used for the prediction of the bending capacity of a metallic pipe with an existing dent on its compression side. The suitable application domain for this formula is λ_l between 0.4 and 5.0, and d_d/t between 0.13 and 2.0. It should be noted that we have not proposed an empirical equation for the critical curvature due to the existence of large scatters during test validation in Section 4. It will be further investigated in the following research of the authors.

7. Conclusion remarks

In this paper, the residual ultimate strength of a dented metallic pipe (D/t of 21.3) subjected to pure bending has been quantitatively investigated based on nonlinear FEM. A numerical model has been developed and validated by test results, capable of predicting residual strength of dented pipe in terms of bending capacity. The effects of dent variables including dent location, dent length (l_d), dent depth (d_d), dent width (w_d) and dent angle (θ_d) have been identified. An empirical formula for predicting the bending capacity of dented pipes accounting for the critical dent parameters has been proposed. Based on the performed work, the following conclusions can be drawn:

- The comparison results between the predictions from the proposed formula and both the test and FEM results show a satisfying fit. It can be used for practice purposes.
- A dent on the compression side of pipe surface has negative effect on its residual strength, whereas the effect is small when it is on the tensile side.
- For dent angle (θ_d), the larger the dent rotation angle is, the smaller the residual ultimate strength will be. It is found that a pipe with a hoop dent (90°) on its compression side has the largest effect on strength.
- For the projected dent length (l'_d) (in 90°), it significantly affects the residual strength of dented metallic pipes, decreasing with the increase of its dimensionless length.
- The dent depth (d_d) significantly affects the residual strength of dented metallic pipes. With the increase of the dent depth, the strength decreases rapidly.
- The dent width(w_d) in pipe longitudinal direction has an insignificant effect on the pipe residual strength.
- With the decrease of D/t ratio, the failure mode of pipes under bending gradually changes from an elastic buckling to an elastic–plastic failure.
- The ovalisation in terms of the lateral displacement in the critical cross-section of dented pipe has an increasing tendency with the increase of dent depth, whereas it is approximately stable with the increase of the dent width.

Acknowledgments

Thanks to the financial support of China Scholarship Council (CSC) [grant number 201406230001]. The funding for the tests provided by Section of Transport Engineering and Logistics, Department of Maritime and Transport Technology, Delft University of Technology, the Netherlands, and School of Transportation, Wuhan University of Technology, PR China, is also appreciated.

Disclosure statement

No potential conflict of interest was reported by the authors.

Funding

China Scholarship Council (CSC) [grant number 201406230001]; Delft University of Technology; Wuhan University of Technology.

ORCID

Jie Cai http://orcid.org/0000-0002-6561-5626
Xiaoli Jiang http://orcid.org/0000-0001-5165-4942
Gabriel Lodewijks http://orcid.org/0000-0002-6466-4346

References

Abaqus613. 2013. Abaqus: User's manual, 6.13. Available from: http://129.97.46.200:2080/v6.13/.

Bai Q, Bai Y., 2014a. Subsea pipeline design, analysis, and installation. Oxford (UK): Gulf Professional Publishing.

Bai Y, Bai Q., 2014b. Subsea pipeline integrity and risk management. Oxford (UK): Gulf Professional Publishing.

Bjørnøy O, Rengård O, Fredheim S, Bruce P, et al., 2000. Residual strength of dented pipelines, DNV test results. In: Proceedings of the 10th International Offshore and Polar Engineering Conference. Seattle (WA): International Society of Offshore and Polar Engineers; p. 182–188.

BSI. 2005. BS7910: guide to methods for assessing the acceptability of flaws in metallic structures. London: British Standards Institution.

Cai J, Jiang X, Lodewijks G., 2016. Residual strength of metallic pipelines subjected to combined loads accounting for impact induced damage. In: Proceedings of the 26th International Offshore and Polar Engineering Conference. St. Jone's: International Society of Offshore and Polar Engineers.

Cai J, Jiang X, Lodewijks G., 2017. Residual ultimate strength of offshore metallic pipelines with structural damage–a literature review. Ships Offshore Struct. 12: 1–19.

Cai J, Jiang X, Lodewijks G, Pei Z, Zhu L., 2017. Experimental investigation of residual ultimate strength of damaged metallic pipelines. In: Proceeding of the 36th International Conference on Offshore Mechanics and Arctic Engineering. Rhodes: American Society of Mechanical Engineers.

Cosham A, Hopkins P., 2004. An overview of the pipeline defect assessment manual (pdam). In: 4th International Pipeline Technology Conference; Belgium: May. p. 9–13.

DNV. 2010. DNV-RP-F111 interference between trawl gear and pipelines. Norway: Det Norske Veritas.

DNV. 2013. DNV-OS-F101 submarine pipeline systems. Norway: Det Norske Veritas.

Es S, Gresnigt A, Vasilikis D, Karamanos S., 2016. Ultimate bending capacity of spiral–welded steel tubes–part i: experiments. Thin-Walled Struct. 102: 286–304.

GB/T 1591., 2008. 低合金高强度结构钢 [High strength low alloy structural steels]. China: Chinese National Standard. Chinese.

Ghaednia H, Das S, Wang R, Kania R., 2015. Effect of operating pressure and dent depth on burst strength of NPS30 linepipe with dent–crack defect. J Offshore Mech Arct Eng. 137(3): 031402-1–031402-8.

Gong S, Ni X, Bao S, Bai Y., 2013. Asymmetric collapse of offshore pipelines under external pressure. Ships Offshore Struct. 8(2): 176–188.

Gresnigt A, Karamanos S, Andreadakis K., 2007. Lateral loading of internally pressurized steel pipes. J Pressure Vessel Technol. 129(4): 630–638.

Hilberink A., 2011. Mechanical behaviour of lined pipe [PhD thesis]. Delft: Delft University of Technology.

Kyriakides S, Corona E., 2007. Mechanics of offshore pipelines. Vol. 1, Buckling and collapse. Oxford: Elsevier.

Lee GH, Seo JK, Paik JK., 2017. Condition assessment of damaged elbow in subsea pipelines. Ships Offshore Struct. 12(1): 135–151.

Macdonald K, Cosham A., 2005. Best practice for the assessment of defects in pipelines–gouges and dents. Eng Fail Anal. 12(5): 720–745.

Manes A, Porcaro R, Ilstad H, Levold E, Langseth M, Børvik T., 2012. The behaviour of an offshore steel pipeline material subjected to bending and stretching. Ships Offshore Struct. 7(4): 371–387.

Mohd MHB, Kim DW, Lee BJ, Kim DK, Seo JK, Paik JK., 2014. On the burst strength capacity of an aging subsea gas pipeline. J Offshore Mech Arct Eng. 136(4): 041402.

Mohd MH, Lee BJ, Cui Y, Paik JK., 2015. Residual strength of corroded subsea pipelines subject to combined internal pressure and bending moment. Ships Offshore Struct. 10(5): 554–564.

Orynyak I., Rozhonyuk, V., Shlapak L., 1999. Residual strength of pipelines with dents. Mater Sci. 35: 689–694.

Paik J, Thayamballi A., 2006. Some recent developments on ultimate limit state design technology for ships and offshore structures. Ships Offshore Struct. 1(2): 99–116.

Pakiding L. 2007. Design criteria for high strength steel joints [dissertation]. Delft: Delft University of Technology.

Park T, Kyriakides S., 1996. On the collapse of dented cylinders under external pressure. Int J Mech Sci. 38(5): 557–578.

Prabu B, Raviprakash A, Venkatraman A., 2010. Parametric study on buckling behaviour of dented short carbon steel cylindrical shell subjected to uniform axial compression. Thin-Walled Struct. 48(8): 639–649.

Ramberg W, Osgood W. 1943. Description of stress–strain curves by three parameters. Technical Note No. 902. Washington (DC): National Advisory Committee for Aeronautics.

Vasilikis D, Karamanos S, Es S, Gresnigt A., 2015. Ultimate bending capacity of spiral–welded steel tubes–part ii: predictions. Thin-Walled Struct. 102: 305–319.

Yang Z, Li H, Guo X, Li H., 2007. Damage assessment in pipeline structures using modal parameter. Ships Offshore Struct. 2(2): 191–197.

Zhang S, Pedersen PT, Ocakli H., 2015. Collisions damage assessment of ships and jack-up rigs. Ships Offshore Struct. 10(5): 470–478.